Journal of Ultrafine Grained and Nanostructured Materials
https://jufgnsm.ut.ac.ir
Vol. 54, No.1, June 2021, pp. 21-28
Print ISSN: 2423-6845 Online ISSN: 2423-6837
DOI: 10.22059/jufgnsm.2021.01.02

Investigation of particle size effect on antibacterial activity of copper ferrite using polyvinylidene fluoride (PVDF) and silicone rubber matrices

Akbar Mirzaei[1], Farzaneh Azadi[2], Reza Peymanfar*[,2], Mona Yektaei[1], Shahrzad Javanshir[1]

[1]Department of chemistry, Iran University of Science and Technology, Tehran, Iran.
[2]Department of Chemical Engineering, Energy Institute of Higher Education, Saveh, Iran.

Recieved: 31 October 2020; Accepted: 13 February 2021
** Corresponding author email: peymanfar@alumni.iust.ac.ir*

ABSTRACT

In this research, the dependence of $CuFe_2O_4$ particle size on the antibacterial properties was investigated. The morphology of the particles was controlled in the presence or lack of glucose as a novel capping agent. Antibacterial properties of the $CuFe_2O_4$ nanoparticles were evaluated using the PVDF or silicon rubber matrices. The crystalline structures of the $CuFe_2O_4$ were confirmed by X-ray diffraction (XRD) patterns. The prepared nanostructures were more dissected using field emission scanning electron microscopy (FE-SEM), Fourier transform infrared (FT-IR), and vibrating sample magnetometer (VSM). Eventually, the copper ferrite particle size effect in PVDF and silicone rubber matrices on the antibacterial activity was investigated. The obtained results revealed significant antibacterial properties for the particles. It was found that decreasing particle size would improve antibacterial properties within both polymeric mediums. This research presents novel separable antibacterial magnetic nanostructure suspended in novel media.

Keywords: *$CuFe_2O_4$, Antibacterial activity, Silicone rubber, Polyvinylidene fluoride (PVDF)*

1. Introduction

Nowadays, antibacterial properties of metals, metal oxides, metal sulphides, as well as composites containing metal structures have attracted substantial attentions. Additionally, nanoscaled materials have been widely used as antibacterial agents [1]. Antibacterial properties of numerous nanostructures such as CuS[2], gentamicin coated iron oxide nanoparticles[3], Ag-related and Cu nanostructures[4, 5], TiO_2-chitosan[6], TaN-Cu[7], Fe_3O_4-Ag [8], ZnO nanostructures and composites[1, 9], etc. have been examined. The achieved results have declared that enhancing the mass fraction of Cu in SiO_2@Cu composite augments the antibacterial activity [10]. As presented by Liu et al., enhancing surface area to volume ratio of copper particles is the key factor to promote its antibacterial properties [7]. Besides, the CuS nanostructure has illustrated intense antibacterial properties[2]. The Cu^+ can react with H_2O_2 from the respiration of the bacterium, creating $OH^\bullet$ and Cu^{2+}. The emerged radicals and Cu^{2+} react with membrane and DNA of bacteria, killing them[11, 12]. The proposed mechanisms can be extended for diverse ions including Fe^{2+} [13]. Moreover, Fe_2O_3 nanoparticles have revealed growth inhibition of bacteria [14]. Phytosynthesis of the Fe_2O_3 nanoparticles demonstrated a proper antibacterial property on Escherichia coli (E. coli) and Staphylococcus aureus (S. aureus)

bacteria[15]. Based on the reported researches, the antibacterial activity of metals and metal oxides including Ag, ZnO, Cu, CuO, Cu_2O, and etc depends on the size, morphology, concentration, shape, and crystalline phase of the solid phase, as well as number and type bacteria. The obtained results attested that the surface area to volume ratio plays the vital role paving the way for antibacterial features. The enhancement of this factor promotes the metal oxide interactions with bacteria at the grain boundaries. The size effect of metal oxide particles on the antibacterial properties has been reported[16]. The obtained results showed that the antibacterial properties on E. coli enhance by diminishing Cu_2O particle size[17]. On the other hand, the recent research has shown that the antibacterial property of CuO has a clear compromise with the particle size. It was found that by reducing the particle size from 26 to 20 nm, the inhibition of bacterial growth E. coli, P. aeruginosa, B. subtilis and S. aureus increases[18]. Interestingly, the antibacterial properties of Fe_3O_4 are improved by augmenting the concentration[18, 19]. Recently, the microwave absorbing properties of the bare or capped $CuFe_2O_4$ nanoparticles using PVDF or silicone rubber mediums have been reported by our research group[20]. Moreover, the size influence on the antibacterial activity of the spinel $CuCr_2O_4$ structure dispersed in PVDF or silicone rubber media was investigated using glucose as a capping agent[21]. It should be noted that there is not any report related to the size-dependent $CuFe_2O_4$ structure on the antimicrobial properties. In this study, glucose was used as a novel organic template and a magnetic antibacterial structure was architected, based on the $CuFe_2O_4$. We have scrupulously investigated the size and medium effect on growth inhibition of bacteria.

2. Experimental

2.1. Precursors and instruments

Chemical precursors including the dimethylformamide (DMF), Fe $(NO_3)_3$ * 9 H_2O, ammonia solution 25%, Cu $(NO_3)_2$ * 3 H_2O, citric acid monohydrate, and glucose were suplied from MEREK, while silicone rubber was provided from ELASTOSIL® M4503. E. coli 1330 and S. aureus 25935 were obtained from Persian Type Culture Collection (PTCC), Iranian Research Organization for Science and Technology (IROST). This study was carried out using FT-IR (Shimadzu 8400 S) and FE-SEM (Tuscan Mira3) to investigate fuctional groups and morphologies. Philips X'Pert MPD used to identify the crystal structure. The magnetic properties of synthesized particles were characterized using IRI Kashan VSM. Eventually, the antibacterial properties of $CuFe_2O_4$ were studied in agar medium (AM) by E. coli and S. aureus.

2.2. Preparation of bare and modified $CuFe_2O_4$ by the sol-gel method

The bare and modified $CuFe_2O_4$ were prepared based on our previous works [20, 22-24]. Briefly, copper and iron nitrate salts (molar ratio of 1 to 2) were dissolved in distilled water. Afterwards, the citric acid (molar ratio of 1 to 1 with cationic metals) was added to the solution. Noteworthy, to prepare modified $CuFe_2O_4$ glucose based on the esterification reaction (molar ratio of 1 to 1 between carboxyl and hydroxyl groups) was used. In the next step, the pH was tuned around 8 by ammonia and then a wet gel was obtained at 80 ° C. Next, the wet gel was dried at 350 °C (for 4 h) and eventually calcined for 3 h at 850 °C.

2.3. Preparation of antibacterial films

The antibacterial films were prepared based on our recent researches [20, 25, 26]. Briefly, PVDF was dissolved in DMF and then $CuFe_2O_4$ (bare or modified) with 35% Wt. (guest/host + guest) was suspended in the aforementioned solution. Eventually, the PVDF composites were molded at 200 °C.

To prepare silicone rubber composites, firstly, $CuFe_2O_4$ particles (bare or modified) were blended in the silicon resin with 35 Wt.% (guest/host (resin + hardener) + guest). Next, the hardener (hardener/resin= 20 Wt.%) was loaded and blended to mold the bare or modified $CuFe_2O_4$/silicone rubber composite. PVDF and silicone rubber were used as polymeric matrices for investigating and comparing their antibacterial properties. Scheme 1 displays the schematic illustration related to the synthetic scenario of the antibacterial composites.

Scheme 1. Schematic illustration related to the synthetic scenario of the antibacterial composites

2.4. Procedure for the antibacterial evaluation

The antibacterial activity of the composites was investigated using 1.5 * 10^8 colony-forming units ($CFU.ml^{-1}$) of bacteria (S. aureus and E.coli) in a Muller Hinton agar medium by diffusion method, for bare and modified $CuFe_2O_4$ composites. The DMF and Tween80 were used to

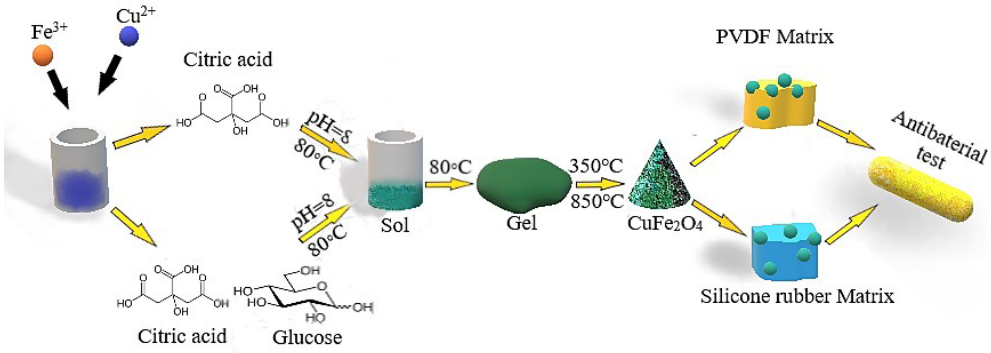

Scheme 1- Schematic illustration related to the synthetic scenario of the antibacterial composites.

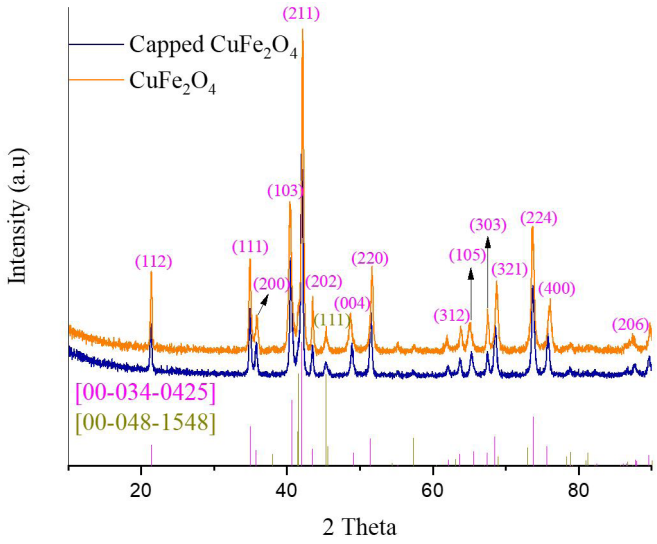

Fig. 1- XRD patterns of the bare and capped nanostructures.

improve the diffusion of the bare and modified $CuFe_2O_4$ composites. Initially, the bare or modified composites (1*1cm) were separately soaked in a solution of Tween80 with 0.05% ($V.V^{-1}$) or DMF and then placed in a culture medium containing bacteria. Also, a saturated suspension of the bare and modified $CuFe_2O_4$/PVDF were separately prepared using the DMF to assess their antibacterial characteristics by the hole-plate diffusion method (height= 1 cm and diameter= 0.5 cm). Afterwards, the culture mediums containing the samples were placed at 4 °C for 2 h and eventually incubated in 37 °C for 24 h.

3. Results and Discussions

3.1. XRD patterns

The crystalline structures of the bare and modified $CuFe_2O_4$ were assessed by XRD technique (Fig. 1). The obtained peaks testified that the tetragonal crystal system of $CuFe_2O_4$ has been synthesized, based on JCPDS: [00-034-0425]. The observed diffraction peak at 2q= 45.27 ° is associated with (111) Bragg reflection, emerged by formed CuO structure (JCPDS: [00-048-1548]) [20, 23, 24, 27].

3.2. FE-SEM micrographs

The FE-SEM micrographs demonstrated that the organic capping agent has changed the morphology of the structures, leading to an enhancement in average size of the particles. The average size of the bare structures was about 250 nm meanwhile it was about 1000 nm for the capped structures. Meanwhile, both particles have the uniform hierarchical structures. The presence of the capping agent due to the enhancing ignition temperature compared to citric acid as well as hydrogen bonding augments average size. On

Table 1- Magnetic parameters of $CuFe_2O_4$ structures

Sample	$CuFe_2O_4$	Modified $CuFe_2O_4$
M_s (emu/g)	25	28
H_c (Oe)	325	154
M_r (emu/g)	11	7

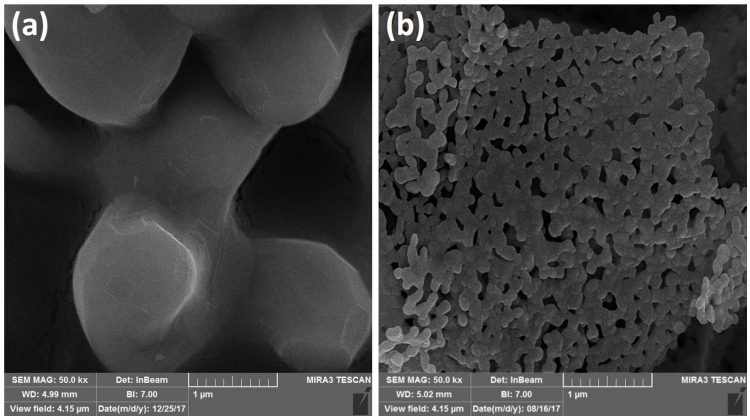

Fig. 2- FE-SEM micrographs of the (a) modified and (b) bare $CuFe_2O_4$.

the other hand, the created polyester, originated from the esterification between carboxylic (from citric acid) and hydroxyl (from glucose) groups can act as a cages, changing the morphology of the particles (Fig. 2). The recent researches have declared that the decomposition temperatures of glucose and sucrose are more than citric acid and loading the sucrose enhances the thermal stability of blended citric acid/sucrose [28-30]. Moreover, the current works have demonstrated that inserting the sucrose or glucose can modify the morphology of the nanoparticles in the presence of citric acid which may be originated from the aforementioned mechanisms [20, 22, 31-33].

3.3. FT-IR spectra

Fig. 3 presents FT-IR spectra of bare and modified $CuFe_2O_4$. The stretching vibration of the adsorbed CO_2 was confirmed by the observed peak at 2337 cm^{-1} [20]. The stretching vibrations of copper ferrite related to the octahedral and tetrahedral sites are shown with the peaks at 423 and 574 cm^{-1}[25, 34]. The obtained parallel absorption bands manifest that the chemical structure of the bare and modified $CuFe_2O_4$ is same; nevertheless, the peak intensity of bare nanoparticles is more than the modified structure that can be generated from its smaller size. The assigned peaks at 1531, 1676, and 3500 cm^{-1} are indexed to the bending and stretching vibrations of the residual -OH groups at the grain boundaries of copper ferrite structures

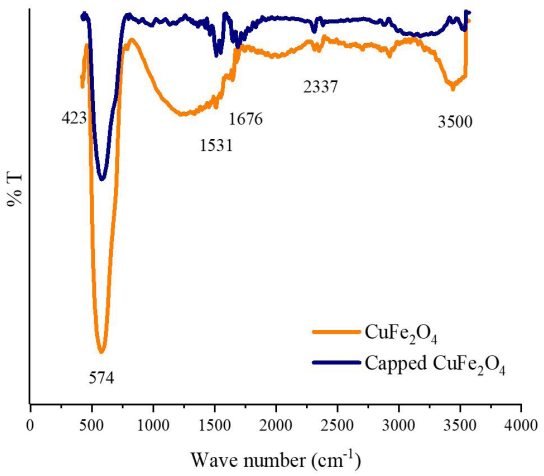

Fig. 3- FT-IR of $CuFe_2O_4$ structures.

as well as hydrogen-bonded H_2O[20, 24, 26]. The achieved spectra attested that there is not any FT-IR peak associated with the organic functional groups of the used precursors, illustrating that all of the impurities have been eliminated after heat treatment [35].

3.4. Magnetic properties

Table 1 exposes the values of the saturation magnetization (M_s), coercivity (H_c), and remanent magnetization (M_r) for bare and modified $CuFe_2O_4$. The hysteresis loops were obtained in the applied field range of −8500 < Oe < +8500 in a vibrating frequency of 25 Hz at the room temperature.

The hysteresis loops exhibited that the M_s of the modified particles were improved. According to the Snoek's law it is clear that, magnetic characteristics are deepened on the size of the structures [36, 37] (Fig. 4).

3.5. Antibacterial evaluation

Figs. 5 and 6 show that the bare and modified $CuFe_2O_4$/silicon rubber soaked in Tween80 (ST) and $CuFe_2O_4$/PVDF evaluated by hole-plate diffusion method have considerable inhibition zone in both polymeric mediums against E.coli and S. aureus. In this study the relationship between the antibacterial property and the particle size was dissected using the $CuFe_2O_4$. It was found that the bare $CuFe_2O_4$ structures demonstrated more antibacterial properties, emerged from their more surface area to volume ratio (Figs. 5 and 6). Although the antibacterial mechanism of the metal oxides is not clear, nevertheless several specific mechanisms have been proposed. The achieved results illustrate that the antibacterial activity of polymer/metal oxide composites is emerged by the activity of metal particles and released metallic ions from the composite. Numerous studies have mentioned that the released ions from polymer/metal oxide composites is the dominant mechanism, bringing antibacterial activity[12, 38]. Additionally, the interactions of the water molecules, from the bacterial medium, at the

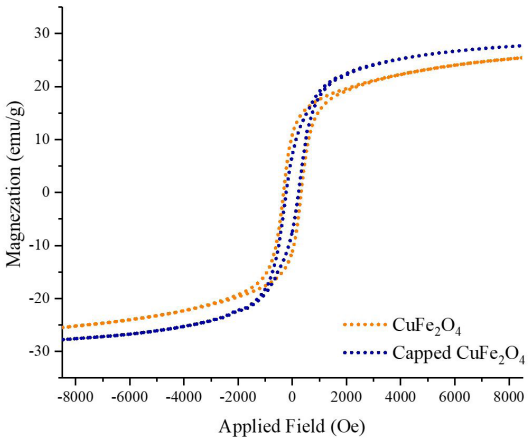

Fig. 4- Hysteresis loops of the capped and bare $CuFe_2O_4$.

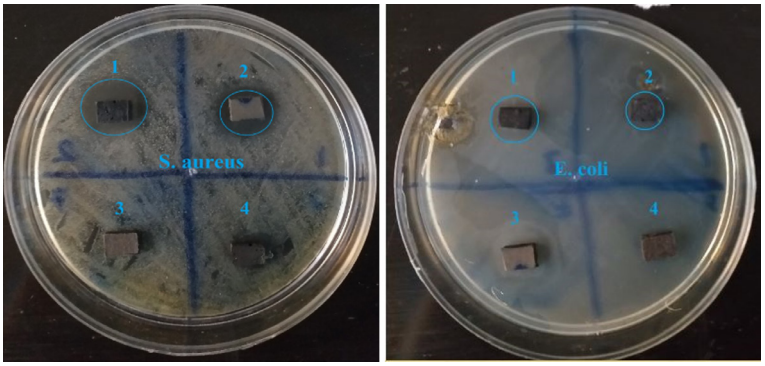

Fig. 5- Antibacterial tests of 1) bare and 2) modified/silicone rubber as well as 3) bare and 4) modified nanoparticles/PVDF ST.

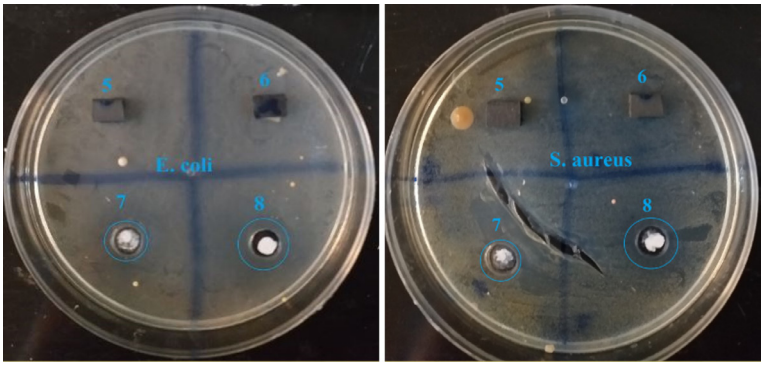

Fig. 6- Antibacterial tests of 5) bare and 6) modified nanoparticles/PVDF SD as well as 7) modified and 8) bare nanoparticles/PVDF evaluated by hole-plate diffusion method.

metal oxide interfaces lead to the corrosion of them releasing metallic ions. The antibacterial characteristics of the $CuFe_2O_4$ suspended in PVDF or silicon rubber media may be derived from its corrosion leading to release Cu^{2+} and Fe^{3+} ions. The produced Cu^{2+} directly interacts with the atoms existing in the bacterium, such as nitrogen, sulfur, and oxygen, which can kill it. This phenomenon realized by the change in the structure and conformation of nucleic acids and proteins of bacteria. Moreover, adsorbed Cu^{2+} on the macromolecules of the bacterial cell distorts them, which the damaged bacterial membrane allows that other ion intake to the bacteria cell[12]. It is well known that alone Fe^{3+} has not any antibacterial activity, but E. coli and S. aureus bacteria can absorb Fe^{3+} and reducing them to Fe^{2+}. It should be noted that produced Fe^{2+} can inhibit bacterial growth through the fenton reaction, based on the reactive oxygen species (ROS)[12, 39]. Particularly, hydrogen peroxide, produced by bacterial aerobic respiration, oxidizes Fe^{2+} to Fe^{3+} developing ROS (OH^- and $OH^\bullet$). The produced ROS reacts with different parts of bacteria such as carbohydrate, protein, and DNA eventually killing bacterium[12, 40]. Interestingly, the soaked PVDF composites did not show any inhibition zone, originated by more dipole interaction of the fluorine atoms within the PVDF mediums compared to the silicone rubber. The $n \rightarrow s^*$ interactions between the fluorine atoms and grain boundaries lead to cover the $CuFe_2O_4$ structures by PVDF confining the interactions between the $CuFe_2O_4$ structures and bacteria. Hence, the $CuFe_2O_4$/PVDF soaked in DMF (SD) and ST did not show any zone of inhibition. Meanwhile, the achieved results refer that by dissolving the $CuFe_2O_4$/PVDF composites in DMF the antibacterial activity of the $CuFe_2O_4$ structures is appeared. More significantly, the obtained results attest that PVDF has no antibacterial activity. Fig. 7 has depicted a column chart of antibacterial activity of the samples.

4. Conclusion

In this study, the bare and modified $CuFe_2O_4$ nanoparticles with tetragonal structure were prepared using the sol-gel method in the absence or presence the glucose as a novel organic capping agent. The XRD patterns confirmed the crystal structure of the obtained copper ferrite nanoparticles and the FT-IR spectra illustrated that the nanoparticles have been synthesized without any organic impurity. Interestingly, the FE-SEM micrographs revealed that the capping agent enhanced the size of the nanoparticles. Moreover, the hysteresis loops illustrated the size effects on magnetic characteristics. Noteworthy, the presented antibacterial results exhibited the influence of the surface area to volume ratio on zone of inhibition. More significantly, the novel separable antibacterial magnetic nanostructure demonstrated inhibition zones with the both PVDF and silicone rubber mediums.

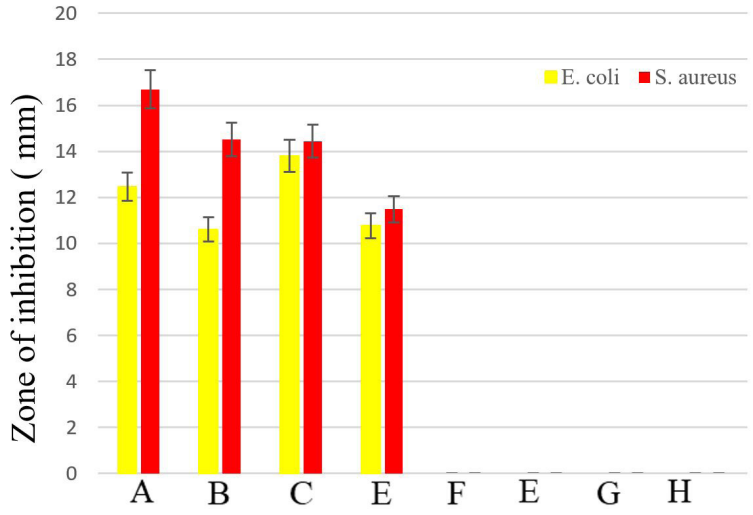

Fig. 7- a column chart of antibacterial activity of A) bare $CuFe_2O_4$/silicone rubber (ST), B) modified $CuFe_2O_4$/ silicone rubber (ST), C) bare $CuFe_2O_4$/ PVDF (hole-plate diffusion method), D) modified $CuFe_2O_4$/ PVDF (hole-plate diffusion method), E) modified $CuFe_2O_4$/ PVDF (SD), F) bare $CuFe_2O_4$/ PVDF (SD), G) bare $CuFe_2O_4$/ PVDF (ST), H) modified $CuFe_2O_4$/ PVDF (ST).

References

1. Alipour A, Javanshir S, Peymanfar R. Preparation, Characterization and Antibacterial Activity Investigation of Hydrocolloids Based Irish Moss/ZnO/CuO Bio-based Nanocomposite Films. Journal of Cluster Science. 2018;29(6):1329-36.
2. Zare Khafri H, Ghaedi M, Asfaram A, Javadian H, Safarpoor M. Synthesis of CuS and ZnO/Zn(OH)2 nanoparticles and their evaluation for in vitro antibacterial and antifungal activities. Applied Organometallic Chemistry. 2018;32(7):e4398.
3. Bhattacharya P, Neogi S. Gentamicin coated iron oxide nanoparticles as novel antibacterial agents. Materials Research Express. 2017;4(9):095005.
4. Ghorbanpour M. Antibacterial activity of porous anodized copper. Journal of Ultrafine Grained and Nanostructured Materials. 2018 Jun 1;51(1):84-9.
5. Garshasbi N, Ghorbanpour M, Nouri A, Lotfiman S. Preparation of Zinc Oxide-Nanoclay Hybrids by Alkaline Ion Exchange Method. Brazilian Journal of Chemical Engineering. 2017;34(4):1055-63.
6. Li J, Xie B, Xia K, Li Y, Han J, Zhao C. Enhanced Antibacterial Activity of Silver Doped Titanium Dioxide-Chitosan Composites under Visible Light. Materials (Basel). 2018;11(8):1403.
7. Liu PC, Hsieh JH, Li C, Chang YK, Yang CC. Dissolution of Cu nanoparticles and antibacterial behaviors of TaN–Cu nanocomposite thin films. Thin Solid Films. 2009;517(17):4956-60.
8. Amarjargal A, Tijing LD, Im I-T, Kim CS. Simultaneous preparation of Ag/Fe3O4 core–shell nanocomposites with enhanced magnetic moment and strong antibacterial and catalytic properties. Chemical Engineering Journal. 2013;226:243-54.
9. Abebe B, Zereffa EA, Tadesse A, Murthy HCA. A Review on Enhancing the Antibacterial Activity of ZnO: Mechanisms and Microscopic Investigation. Nanoscale research letters. 2020;15(1):190-.
10. Zhang N, Gao Y, Zhang H, Feng X, Cai H, Liu Y. Preparation and characterization of core–shell structure of SiO2@Cu antibacterial agent. Colloids and Surfaces B: Biointerfaces. 2010;81(2):537-43.
11. Konieczny J, Rdzawski Z. Antibacterial properties of copper and its alloys. Archives of Materials Science and Engineering. 2012;56(2):53-60.
12. Palza H. Antimicrobial polymers with metal nanoparticles. International journal of molecular sciences. 2015;16(1):2099-116.
13. Ubale AU, Belkhedkar MR. Size Dependent Physical Properties of Nanostructured α-Fe2O3 Thin Films Grown by Successive Ionic Layer Adsorption and Reaction Method for Antibacterial Application. Journal of Materials Science & Technology. 2015;31(1):1-9.
14. Khataminejad MR, Mirnejad R, Sharif M, Hashemi M, Sajadi N, Piranfar V. Antimicrobial Effect of Imipenem-Functionalized Fe(2)O(3) Nanoparticles on Pseudomonas aeruginosa Producing Metallo β-lactamases. Iran J Biotechnol. 2015;13(4):43-7.
15. Irshad R, Tahir K, Li B, Ahmad A, R. Siddiqui A, Nazir S. Antibacterial activity of biochemically capped iron oxide nanoparticles: A view towards green chemistry. Journal of Photochemistry and Photobiology B: Biology. 2017;170:241-6.
16. Stanić V, Tanasković SB. Antibacterial activity of metal oxide nanoparticles. Nanotoxicity: Elsevier; 2020. p. 241-74.
17. Xiong L, Yu H, Nie C, Xiao Y, Zeng Q, Wang G, et al. Size-controlled synthesis of Cu2O nanoparticles: size effect on antibacterial activity and application as a photocatalyst for highly efficient H2O2 evolution. RSC Advances. 2017;7(82):51822-30.
18. Azam A, Ahmed AS, Oves M, Khan MS, Memic A. Size-dependent antimicrobial properties of CuO nanoparticles against Gram-positive and -negative bacterial strains. Int J Nanomedicine. 2012;7:3527-35.
19. Gabrielyan L, Hovhannisyan A, Gevorgyan V, Ananyan M, Trchounian A. Antibacterial effects of iron oxide (Fe3O4) nanoparticles: distinguishing concentration-dependent effects with different bacterial cells growth and membrane-associated mechanisms. Applied Microbiology and Biotechnology. 2019;103(6):2773-82.
20. Peymanfar R, Azadi F. Preparation and identification of bare and capped CuFe2O4 nanoparticles using organic template and investigation of the size, magnetism, and polarization on their microwave characteristics. Nano-Structures & Nano-Objects. 2019;17:112-22.
21. Mirzaei A, Peymanfar R, Khodamoradipoor N. Investigation of size and medium effects on antimicrobial properties by CuCr2O4 nanoparticles and silicone rubber or PVDF. Materials Research Express. 2019;6(8):085412.
22. Peymanfar R, Rahmanisaghieh M. Preparation of neat and capped BaFe2O4 nanoparticles and investigation of morphology, magnetic, and polarization effects on its microwave and optical performance. Materials Research Express. 2018;5(10):105012.
23. Ghazvini M, Maddah H, Peymanfar R, Ahmadi MH, Kumar R. Experimental evaluation and artificial neural network modeling of thermal conductivity of water based nanofluid containing magnetic copper nanoparticles. Physica A: Statistical Mechanics and its Applications. 2020;551:124127.
24. Peymanfar R, Azadi F. La-substituted into the CuFe2O4 nanostructure: a study on its magnetic, crystal, morphological, optical, and microwave features. Journal of Materials Science: Materials in Electronics. 2020;31(12):9586-94.
25. Peymanfar R, Javanshir S, Naimi-Jamal MR, Cheldavi A, Esmkhani M. Preparation and Characterization of MWCNT/Zn0.25Co0.75Fe2O4 Nanocomposite and Investigation of Its Microwave Absorption Properties at X-Band Frequency Using Silicone Rubber Polymeric Matrix. Journal of Electronic Materials. 2019;48(5):3086-95.
26. Peymanfar R, Afghahi SSS, Javanshir S. Preparation and Investigation of Structural, Magnetic, and Microwave Absorption Properties of a SrAl1.3Fe10.7O19/Multiwalled Carbon Nanotube Nanocomposite in X and Ku-Band Frequencies. Journal of Nanoscience and Nanotechnology. 2019;19(7):3911-8.
27. Ethiraj AS, Kang DJ. Synthesis and characterization of CuO nanowires by a simple wet chemical method. Nanoscale research letters. 2012;7(1):70-.
28. Zhao Z, Sakai S, Wu D, Chen Z, Zhu N, Huang C, et al. Further Exploration of Sucrose-Citric Acid Adhesive: Investigation of Optimal Hot-Pressing Conditions for Plywood and Curing Behavior. Polymers (Basel). 2019;11(12):1996.
29. Savi LK, Dias MCGC, Carpine D, Waszczynskyj N, Ribani RH, Haminiuk CWI. Natural deep eutectic solvents (NADES) based on citric acid and sucrose as a potential green technology: a comprehensive study of water inclusion and its effect on thermal, physical and rheological properties. International Journal of Food Science & Technology. 2018;54(3):898-907.
30. Ma Z, Zhang H, Yang Z, Zhang Y, Yu B, Liu Z. Highly mesoporous carbons derived from biomass feedstocks templated with eutectic salt ZnCl2/KCl. J Mater Chem A. 2014;2(45):19324-9.
31. Peymanfar R, Fazlalizadeh F. Microwave absorption performance of ZnAl2O4. Chemical Engineering Journal. 2020;402:126089.
32. Peymanfar R, Ramezanalizadeh H. Sol-gel assisted synthesis

of CuCr2O4 nanoparticles: An efficient visible-light driven photocatalyst for the degradation of water pollutions. Optik. 2018;169:424-31.
33. Peymanfar R, Javanshir S, Naimi-Jamal MR, Cheldavi A. Preparation and identification of modified La0.8Sr0.2FeO3 nanoparticles and study of its microwave properties using silicone rubber or PVC. Materials Research Express. 2019;6(7):075004.
34. Peymanfar R, Norouzi F, Javanshir S. A novel approach to prepare one-pot Fe/PPy nanocomposite and evaluation of its microwave, magnetic, and optical performance. Materials Research Express. 2018;6(3):035024.
35. Peymanfar R, Javidan A, Selseleh-Zakerin E. Preparation of modified SrAl 1.3 Fe 10.7 O 19 nanostructures and evaluation of size influence on its optical and magnetic properties. Micro & Nano Letters. 2020;15(11):759-63.
36. Acher O, Dubourg S. Generalization of Snoek's law to ferromagnetic films and composites. Physical Review B. 2008;77(10).
37. Snoek JL. Gyromagnetic Resonance in Ferrites. Nature. 1947;160(4055):90-.
38. Delgado K, Quijada R, Palma R, Palza H. Polypropylene with embedded copper metal or copper oxide nanoparticles as a novel plastic antimicrobial agent. Letters in Applied Microbiology. 2011;53(1):50-4.
39. Yan J, Qian L, Gao W, Chen Y, Ouyang D, Chen M. Enhanced Fenton-like Degradation of Trichloroethylene by Hydrogen Peroxide Activated with Nanoscale Zero Valent Iron Loaded on Biochar. Scientific reports. 2017;7:43051-.
40. Sun H-Q, Lu X-M, Gao P-J. The Exploration of the Antibacterial Mechanism of FE(3+) against Bacteria. Braz J Microbiol. 2011;42(1):410-4.